



The CIFIST 3D model atmosphere grid

H.-G. Ludwig^{1,2}, E. Caffau², M. Steffen³, B. Freytag^{1,2,4}, P. Bonifacio^{1,2,5}, and A. Kučinskas^{6,7}

¹ CIFIST – Marie Curie Excellence Team

² GEPI – Observatoire de Paris, CNRS, Université Paris Diderot, 92195 Meudon, France

³ Astrophysikalisches Institut Potsdam, An der Sternwarte 16, 14482 Potsdam, Germany

⁴ CRAL – UMR 5574 CNRS, Université de Lyon, École Normale Supérieure de Lyon, 46 allée d'Italie, 69364 Lyon Cedex 07, France

⁵ INAF – Osservatorio Astronomico di Trieste, via Tiepolo 11, 34143 Trieste, Italy

⁶ Institute of Theoretical Physics and Astronomy, Goštauto 12, Vilnius LT-01108, Lithuania

⁷ Vilnius University Astronomical Observatory, Čiurlionio 29, Vilnius LT-03100, Lithuania

Abstract. Grids of stellar atmosphere models and associated synthetic spectra are numerical products which have a large impact in astronomy due to their ubiquitous application in the interpretation of radiation from individual stars and stellar populations. 3D model atmospheres are now on the verge of becoming generally available for a wide range of stellar atmospheric parameters. We report on efforts to develop a grid of 3D model atmospheres for late-type stars within the CIFIST Team at Paris Observatory. The substantial demands in computational and human labor for the model production and post-processing render this apparently mundane task a challenging logistic exercise. At the moment the CIFIST grid comprises 77 3D model atmospheres with emphasis on dwarfs of solar and sub-solar metallicities. While the model production is still ongoing, first applications are already worked upon by the CIFIST Team and collaborators.

Key words. Stars: abundances – Stars: atmospheres – hydrodynamics – convection – radiative transfer

1. The simulation code

The 3D simulations were performed with the radiation-hydrodynamics code CO⁵BOLD (Freytag, Steffen, & Dorch 2002; Wedemeyer et al. 2004). The code solves the time-dependent equations of compressible hydrodynamics coupled to radiative transfer in a constant gravity field in a Cartesian computational domain which is representative of a volume located at the stellar surface. The

equation of state takes into consideration the ionization of hydrogen and helium, as well as the formation of H₂ molecules according to Saha-Boltzmann statistics. Relevant thermodynamic quantities – in particular gas pressure and temperature – are tabulated as a function of gas density and internal energy. The multi-group opacities used by CO⁵BOLD are based on monochromatic opacities stemming from the MARCS stellar atmosphere package (Gustafsson et al. 2008) provided as function of gas pressure and temperature with high

Send offprint requests to: H.-G. Ludwig

wavelength resolution. For the calculation of the opacities solar elemental abundances according Grevesse & Sauval (1998) are assumed with the exception of CNO for which values close to the recommendation of Asplund (2005) are adopted (specifically, A(C)=8.41, A(N)=7.80, A(O)=8.67).

2. Model set-up

We typically used a number of $140 \times 140 \times 150$ points for the hydrodynamical grid. The wavelength dependence of the radiation field was represented by 5 multi-group bins in the case of solar metallicity, and 6 bins at sub-solar metallicities following the procedures laid out by Nordlund (1982); Ludwig (1992); Ludwig, Jordan, & Steffen (1994); Vögler, Bruls, & Schüssler (2004). For test purposes we calculated a few models using 12 bins. The sorting into wavelength groups was done applying thresholds in logarithmic Rosseland optical depth $\{+\infty, 0.0, -1.5, -3.0, -4.5, -\infty\}$ for the 5-bin, and $\{+\infty, 0.1, 0.0, -1.0, -2.0, -3.0, -\infty\}$ for the 6-bin schemes. In the case of 12 bins we used as thresholds $\{+\infty, 0.15, 0.0, -0.75, -1.5, -2.25, -3.0, -3.75, -4.5, -\infty\}$; in addition, the first three continuum-like bins were split each into 2 bins according to wavelength at 550, 600, and 650 nm. In all but one bin a switching between Rosseland and Planck averages was performed at a band-averaged Rosseland optical depth of 0.35; in the bin gathering the largest line opacities the Rosseland mean opacity was used throughout. The decisions about number of bins, and sorting thresholds are motivated by comparing radiative fluxes and heating rates obtained by the binned opacities in comparison to the case of high wavelength resolution.

We constructed 3D starting models by scaling existing 3D models according to 1D standard stellar structure models. The 1D models provided scaling factors for thermodynamic, kinematic, and geometrical properties to modified T_{eff} , $\log g$, and metallicity. Points of the same optical depth and same pressure relative to the surface pressure were considered associated between the original and scaled

model, in the optically thin and thick regions, respectively. Empirically, the scaling procedure works particularly reliably if the scaling is performed along lines of constant entropy jump in the $T_{\text{eff}}\text{-}\log g$ -plane (see, e.g., Ludwig, Freytag, & Steffen 1999).

At given T_{eff} and $\log g$ we kept the computational domain the same for each metallicity. Since the models were intended to serve as atmosphere models for spectral synthesis calculations, a minimum extent of the computational domain to $\log \tau_{\text{Ross}} = -6$ was always required. The overall philosophy was to keep the model set-up – in a relative sense – solar-like. We required a minimum time interval over which the model could be considered as relaxed which corresponded to an equivalent of one hour in a solar model.

3. Model calculations and monitoring

The majority of the simulation runs was conducted on a dedicated Linux cluster of 14 double-processor, double-core nodes running one model per node making use of OpenMP parallelization. A main-sequence run is completed in 1–2 months (wall clock time). More CPU demanding giant models were calculated on an IBM SP5 at the Italian CINECA supercomputing center, and in addition on machines at the Institute of Theoretical Physics and Astronomy of Vilnius University (Lithuania). Running up to 20 hydrodynamical models in parallel made it necessary to facilitate the monitoring of simulation runs. For this purpose we developed an automatic procedure producing diagnostic plots in HTML-format depicting the evolution of the thermal, flux, granulation pattern, and oscillatory properties of a model. Figure 1 shows examples of granulation patterns at different metallicity.

4. Snapshot selection and auxiliary data.

After completion of a model run a sub-set of snapshots is selected for spectral synthesis purposes. The selection is guided by the requirement that the statistics of the sub-sample should closely resemble the statistics of the

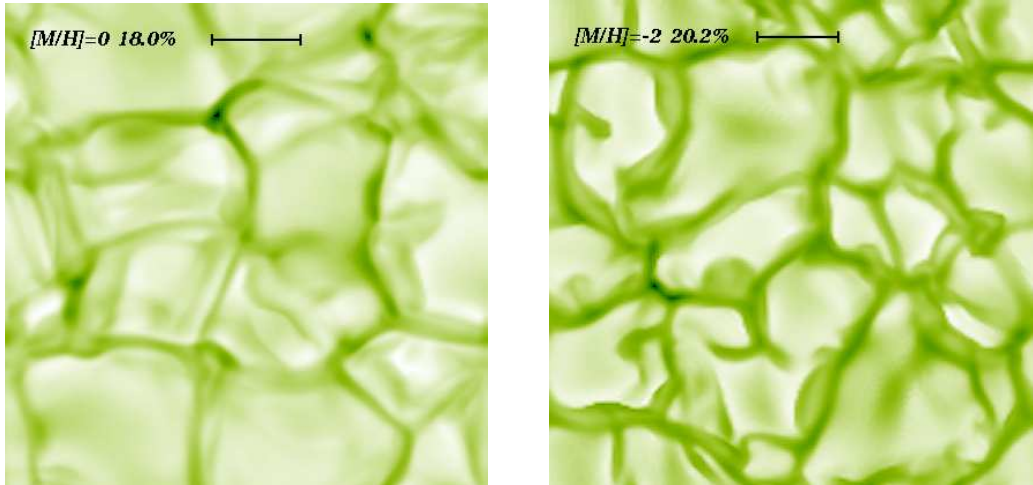


Fig. 1. Typical snapshots of the emergent bolometric intensity (false color representation) from two runs at $T_{\text{eff}}=5000 \text{ K}$, $\log g=2.5$ and metallicities $[M/H]=0$ and -2 . The metallicity, the relative RMS intensity contrast of the image and a scale of 10 times the pressure scale height at $\tau = 1$ are given in each frame.

whole run. In particular, the statistics of fluctuation in velocity and emergent flux should be preserved. The selection is done for reducing the amount of necessary calculations since 3D spectral synthesis calculations are computationally demanding. The selected data is augmented by basic information about mean model properties, and 1D standard atmosphere models which exactly share the atmospheric parameters with the 3D run.

5. Grid completeness and computational costs

At the moment 77 non-solar 3D models have been completed (see Fig. 2). On top of this number we calculated a series of solar models and test models with more detailed (12 bins) radiative transfer. Due to a combination of specific needs for projects and computational costs most models were produced for dwarfs and sub-giants. Figure 3 illustrates the approximate computational costs – i.e., the demand in CPU time – of a model run; the symbol diameter is proportional to the quantity $(\Delta t/\Delta t_{\text{CFL}})^{-0.5}$ where Δt is the typical timestep of a model run, and Δt_{CFL} the Courant-Friedrichs-Levy time. Metallicity generally plays no dominant role for the com-

putational cost. The computational cost rises significantly towards the red giant branch, and towards higher effective temperatures. This basically reflects the decrease of the radiative time scale relative to Δt_{CFL} leading to a reduction of the overall time step.

6. Thoughts for a next generation 3D grid

At present the realism of 3D model atmospheres is limited by the approximations necessary to keep the radiative transfer tractable. Consequently, in next generation grids much effort will be put in refining the radiative transfer. This will be accompanied by a – likely modest – increase in spatial resolution. A perhaps less obvious property should be a higher degree of homogeneity among the models. A global strategy for designing the computational grid is desirable which takes into consideration the physical structure and constraints given by the numerics. This also relates to the way opacities are grouped. A global strategy ensures an increased differential accuracy of properties among models (e.g., granulation contrast, granular scale, equivalent mixing-length parameter, equivalent width of synthetic lines, etc.). This process will benefit from the already

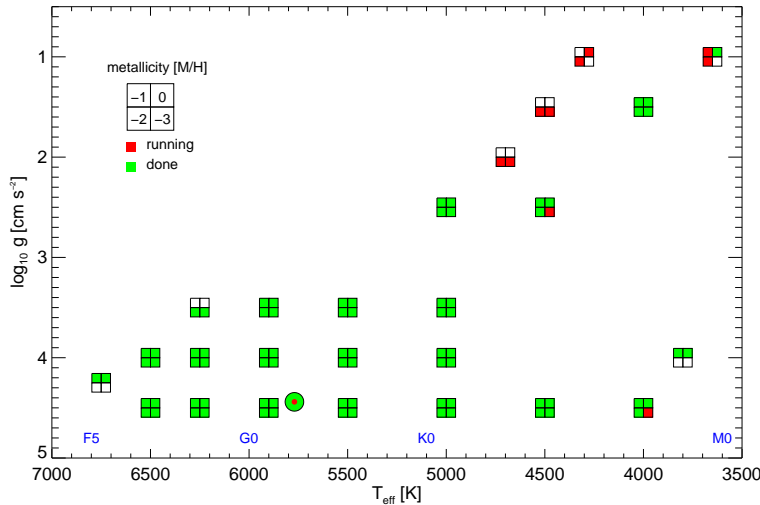


Fig. 2. Status of the model production for the CIFIST grid. Symbols mark the location of a model in the T_{eff} - $\log g$ -plane. Green (gray) color indicates completed model runs, red (black) ongoing calculations. Each square is split into four sub-squares indicating solar, 1/10, 1/100, and 1/1000 of solar metallicity. The solar position is indicated by the round symbol.

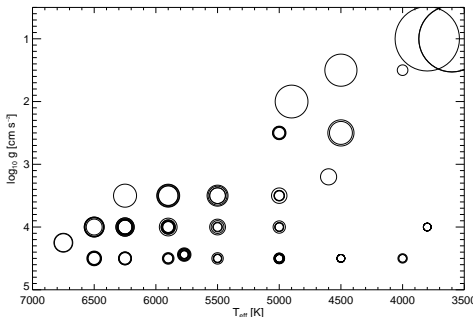


Fig. 3. Approximate computational model cost. The surface area of a circles depicts the approximate compute time of a model run. For details see text.

existing 3D models. If grid completeness is important the computational cost of giants necessitates to include them in the production early. Last but not least dedicated efforts are necessary to make the computational results accessible to the broader astronomical community. Extensive tables of synthetic colors and spectra are the obvious data products which need to be delivered.

Acknowledgements. BF, EC, HGL, and PB acknowledge support from EU contract MEXT-CT-2004-014265 (CIFIST).

References

- Asplund, M. 2005, *ARA&A*, 43, 481
- Freytag, B., Steffen, M., & Dorch, B. 2002, *AN*, 323, 213
- Grevesse, N., & Sauval, A. J. 1998, *SSRv*, 85, 161
- Gustafsson, B., Edvardsson, B., Eriksson, K., Jørgensen, U. G., Nordlund, Å., & Plez, B. 2008, *A&A*, 486, 951
- Ludwig, H.-G. 1992, PhDT, University of Kiel
- Ludwig, H.-G., Jordan, S., & Steffen M. 1994, *A&A*, 284, 105
- Ludwig, H.-G., Freytag, B., & Steffen, M. 1999, *A&A*, 346, 111
- Nordlund, Å. 1982, *A&A*, 107, 1
- Vögler, A., Bruls, J. H. M. J., & Schüssler, M. 2004, *A&A*, 421, 741
- Wedemeyer, S., Freytag, B., Steffen, M., Ludwig, H.-G., & Holweger, H. 2004, *A&A*, 414, 1121